American Mineralogist, Volume 61, pages 74–87, 1976

The crystal structure of bredigite and the genealogy of some alkaline earth orthosilicates

PAUL BRIAN MOORE AND TAKAHARU ARAKI

Department of the Geophysical Sciences, The University of Chicago
Chicago, Illinois 60637

Abstract

Bredigite, (Ca, Ba)$Ca_{13}Mg_2[SiO_4]_8$, $Z = 2$, $a = 10.909(9)$Å, $b = 18.34(1)$Å, $c = 6.739(9)$Å, space group $P2nn$, possesses a crystal structure based on a new kind of pinwheel arrangement. $R(hkl) = 0.108$ ($R_w(hkl) = 0.059$) for 1977 independent reflections.

The space group genealogy for bredigite is: $P2nn \rightarrow Pmnn \rightarrow Pmcb \rightarrow Cmcm \rightarrow P6_3/mmc$. Its idealized arrangement is based on $Pmcb$, $a' = a/2$, $b' = b$, $c' = c$, but ordering of Ba^+ and minor Mn^{2+} leads to $Pmnn$ with $a' = a$. Tilting of the tetrahedra lowers the symmetry to $P2nn$.

It is proposed that bredigite is an ordered Ca:Mg compound with a probable composition range between $Ca_{14}Mg_2[SiO_4]_8$ and $BaCa_{13}Mg_2[SiO_4]_8$. The ideal polyhedral formula is $X^{[12]}X_2^{[9]}Y_4^{[10]}M^{[6]}[TO_4]_4$, where X and Y are large polyhedra, M is the octahedron and T the tetrahedron. Evidence, based on combinatorial analysis and calculated powder patterns, suggests that proper definitions of phases in the system BaO–CaO–MgO–SiO_2 require careful single crystal studies.

Introduction

Bredigite—an important phase in the crystal chemistry of cements, clinkers, slags, and fertilizers—has fostered contention among silicate scientists since its original recognition as a discrete species. In the system CaO–MgO–SiO_2, Nature has been particularly perverse in Her choice of what shall be deemed stable. These compounds share all the problems encountered in substructure-superstructure relations, twinning, exsolution, order-disorder, and grotesque stoichiometry. We hope that some questions may be answered in this study but we fear that just as many answers in the earlier studies must be questioned. In particular, detailed single crystal studies are required—and urgently needed—to properly establish the relationships between composition and stability among the phases.

Experimental

The type specimen of Middlesbrough spiegeleisen slag described by Tilley and Vincent (1948) (University of Cambridge specimen number 47706) was kindly placed at our disposal by Professor S. O. Agrell. The bredigite occurs as long prismatic crystals with hexagonal cross-section up to 2 mm in length parallel to the c axis, which project into the cavities of the melilite groundmass. Twinning on (110) occurs for most of the crystals but is surficially concealed owing to the pseudohexagonal subcell. Several crystals were extracted from the cavities; the sixth crystal examined by X-ray single crystal photography was free from twinning but showed the persistent extra diffuse reflections which Douglas (1952) attributed to the presence of the trigonal phase. This phase, also an alkaline earth orthosilicate, possesses $a = 5.46$Å, ($b = a\sqrt{3} = 9.46$Å), $c = 6.76$Å and is oriented with its a^* and b^* reciprocal lattice vectors parallel to those of bredigite. At low angles, the reflections of the trigonal phase severely overlap those hkl reflections of bredigite for which (h, $k = 2n$), $h + k = 4n$. The crystal selected for complete structure analysis was a symmetrical prism $0.12 \times 0.12 \times 0.20$ mm in dimension. The cell data, obtained from calibrated precession photographs, are $a = 10.909(9)$Å, $b = 18.34(1)$Å, $c = 6.739(9)$Å and the extinction criteria are compatible with the space groups $Pmnn$ or $P2nn$, confirming the observations of Douglas (1952).

The crystal was mounted parallel to its c axis on a PAILRED automated diffractometer utilizing graphite monochromatized Mo$K\alpha_1$ ($\lambda = 0.70926$Å) radiation, $2\theta_{max} = 60°$, and the data were gathered from the $l = 0$ through the $l = 9$ levels. Other salient details: scan speed $1°\text{min}^{-1}$, background counting times 20 sec, scan ranges from 3.6° to 5.2° (the latter at higher levels). Reflections in the blind region of the apparatus were photographically estimated but not in-

cluded in the ensuing refinements of the structure. Owing to the favorable size, shape, and low linear absorption coefficient ($\mu = 30.0\ cm^{-1}$), correction for absorption was not considered necessary. Individual reflections were weighted based on background counting errors, long term source fluctuations, and crystal tilt (maximum deviation = 0.1° from ideal alignment). The intensities whose I_o were within $2\sigma(I)$ of zero were set $I_o = \sigma(I)$. Finally, the equivalent reflections I_o (hkl) and $I_o(\bar{h}kl)$ were averaged, and conventional geometrical conversion to F_o led to 2039 independent reflections in the data set.

Solution of the structure and its refinement

Solution of the bredigite structure was difficult because, like other calcium orthosilicates, a pronounced pseudohexagonal subset predominated in the structure factor data set whereas the weaker reflections held the key to the structure. At first, we assumed the centrosymmetric space group *Pmnn* and adopted the model structure featured as Figure 11 in Moore (1973). This model was in qualitative agreement with the three-dimensional Patterson synthesis, $P(uvw)$. We then proceeded to adopt the ideal cation coordinates from that model and used them for input into the β-synthesis (see Ramachandran and Srinivasan, 1970). The first synthesis provided the general outline of the structure, including all oxygen atoms, and gave clues to the real distortions away from the initial ideal model. A trial least-squares refinement of all atoms in the structure led to $R = 0.50$, the most pronounced discrepancies appearing for hkl, $h = 2n + 1$. Noting that a substructure occurs for bredigite with $a' = a/2$, it was decided that the true combination of pinwheels in the real structure was not isomorphic to the proposed model but was based on distortions of an ideal model with cell parameters $a' = a/2$, $b' = b$, $c' = c$. Search for "ghost" residuals in the β-synthesis led to the proposition that the ideal structure was in fact based on space group *Pmcb* with the cell parameters as stated above. Thus, *Pmnn* is a geometrical distortion of *Pmcb*, requiring a doubling of the a' axis.

The problem then reduced to seeking out the correct distortions leading to the real structure: on combinatorial grounds, there were some 76 possibilities. A new β-synthesis, however, provided sufficient information to permit solution of the actual distortions in the structure leading to the true bredigite cell. Two cycles of least-squares refinement led to $R = 0.33$. At this stage, it was observed that atoms restricted to special positions on the mirror plane were misbehaving; their electron densities were variously split across the mirror plane or merged into broad ellipsoidal contours. The only recourse was to assume that the space group was indeed non-centrosymmetric, *P2nn*. However, we were plagued with the proper choice of further distortion since a decision had to be made to select either (xyz) or ($\bar{x}yz$) when referred to the centrosymmetric map. Appeal was made to the $h0l$ reflections since these were most seriously affected by the absence of the reflection planes. A sufficient number of correct atom positions were recovered to allow proper phasing of the bulk of the weak-to-moderate reflections. Two more β-syntheses led to the correct solution of the structure.

At this stage, some reflections of the type hkl (h, $k = 2n$), $h + k = 4n$ with $F_o \gg F_c$ were eliminated from the refinement since these were contributions from both the bredigite and a part of the trigonal phase structures. Careful inspection for unsymmetrical backgrounds on the recorded data led to rejection of 62, mostly low angle, reflections which exhibited contamination from the trigonal phase. The actual bredigite composition was then adopted for assessment of site populations, and we considered as an initial composition the cell contents suggested by Tilley and Vincent (1948) after renormalization: $Ca_{24.6}Ba_{1.2}Mg_{4.8}Mn_{1.4}[SiO_4]_{16}$. In the earlier study, the divalent metal oxide components sum to 33.1 RO per 16 SiO_2 and we recalculated the contents of the large cations assuming $\sum RO = 32$. We proposed that Ba would substitute for Ca at those sites with large average interatomic distance, and Mn for Mg at the octahedral sites. Scattering curves were prepared for Ca^{2+}, Ba^{2+}, Mn^{2+}, Mg^{2+}, Si^{4+}, and O^{1-} from Cromer and Mann (1968), and refinement of mixed cation distributions over equivalent sites was facilitated by a local modification of a least-squares program reported by Finger (1969). Anomalous dispersion correction for Ca, Ba, Mn, and Mg was adopted from Cromer and Liberman (1970) and the coefficient of secondary extinction correction was refined according to Zachariasen (1968).

The distributions of Ba^{2+} and Mn^{2+} in the crystal were further suggested by refining the multipliers for the large cations based on the scattering curve for Ca^{2+}. Four independent sites, $X(11)$, $M(11)$, $M(12)$ and $Y(11)$, required mixed scattering curves. Bond distances suggested $X(11)$ = (Ca, Ba); $M(11)$, $M(12)$ = (Mg, Mn); and $Y(11)$ = (Ca, Mg). For the last site, the substitution of Mg for Ca was weak.

Our full-matrix least-squares scale factor, site population, isotropic thermal-vibration parameter and atomic-coordinate parameter refinements proceeded

TABLE 1. Dependence of $R(hkl)$ and $R_w(hkl)$ on F_{obs} for Bredigite

	All Reflections				Rejected Reflections Excluded			
	|F(obs)|	Number	R(hkl)	R_w(hkl)	|F(obs)|	Number	R(hkl)	R_w(hkl)
Above	0.0	2039	0.123	0.133	0.0	1977	0.108	0.059
"	12.0	1569	.107	.130	12.0	1507	.088	.051
"	36.0	704	.077	.130	36.0	646	.045	.037
"	72.0	242	.075	.083	72.0	206	.035	.029

from a local modification of the ORFLS program of Busing, Martin, and Levy (1962) and included options for bond distance calculations as well. At the final two cycles, anisotropic thermal vibration parameter refinement was selected for the alkaline earth cations but the silicon cations and the oxygen anions were refined as isotropic species. The results in R and R_w, where

$$R = \frac{\Sigma \, ||F_o| - |F_c||}{\Sigma \, |F_o|} \quad \text{and}$$

$$R_w = \left[\frac{\Sigma_w(|F_o| - |F_c|)^2}{\Sigma_w \, |F_o|^2}\right]^{1/2}$$

with $w = \sigma^{-2}$ of $|F_o|$, are summarized in Table 1. The coefficient of secondary extinction refined to $c_o = 1.2(2) \times 10^{-6}$ and the scale factor $s = 0.630(3)$. Final atomic coordinate parameters, site populations, and (equivalent) isotropic thermal vibration parameters are given in Table 2, anisotropic thermal vibration for the alkaline earth cations in Table 3, the r.m.s. displacements and orientations of these ellipsoids in Table 4, and the structure factor data in Table 5.[1] Table 6 presents selected bond distances and bond angles used in the ensuing discussion on the structure.

In toto, there were one scale factor, one extinction coefficient, four site population parameters, eighty-one atomic coordinate parameters, twenty isotropic thermal vibration parameters and fifty-two anisotropic thermal vibration parameters giving 159 varied parameters in all. This affords a data: variable parameter ratio of about 12:1.

Table 1 shows that R_w for the refinement with rejected reflections is pleasingly low; this situation doubtless arises from the large number of very weak reflections; over two-thirds of the full data set (those reflections less than 36) would be classed as weak reflections. Exclusion of 62 reflections is certainly justified since these were shown to be contributions by the trigonal phase as well, and are starred in Table 5. Since we did not fully integrate over the contributions by the trigonal phase and since the mosaic spreads between the two phases are substantially different, it is difficult to estimate what fraction of the crystal is made up of the trigonal phase. On the basis of film measurements, we estimate it to be less than 20 percent by volume. Mention should be made of the refined site populations in bredigite and those suggested by the chemical analy-

TABLE 2. Bredigite Atomic Coordinate Parameters and (Equivalent) Isotropic Thermal Vibration Parameters*

Atom	x	y	z	B(Å^2)
X(11)	0.0000	0.0000	0.0000	1.6
X(12)	.5016(11)	.0000	.0000	1.5
X(21)	.2362(6)	.2284(2)	-.0003(4)	0.7
X(22)	.7728(6)	.2272(2)	.0056(4)	1.1
M(11)	-.0003(9)	.5000	.0000	0.7
M(12)	.5002(12)	.5000	.0000	0.4
Y(11)	.2564(7)	.4103(2)	.1540(4)	1.3
Y(12)	.7556(7)	.4119(2)	.1614(4)	1.0
Y(21)	.0081(8)	.1722(1)	.3310(2)	1.2
Y(22)	.5061(7)	.1654(1)	.3008(2)	1.4
Si(11)	.7542(8)	.0811(3)	.2188(5)	1.0(1)
O(11-1)	.6388(15)	.0259(8)	.2695(18)	2.4(3)
O(11-1m)	.8681(11)	.0495(6)	.3444(14)	1.5(2)
O(11-2)	.7196(12)	.1605(7)	.3054(16)	1.1(2)
O(11-3)	.7885(15)	.0883(8)	-.0081(19)	2.1(3)
Si(12)	.2594(8)	.0798(2)	.2199(5)	0.7(1)
O(12-1)	.1285(13)	.0609(7)	.3311(16)	2.2(2)
O(12-1m)	.3626(11)	.0241(6)	.2900(14)	0.9(2)
O(12-2)	.2923(13)	.1592(8)	.3233(18)	1.7(2)
O(12-3)	.2294(13)	.0913(7)	-.0103(16)	1.1(2)
Si(21)	.0037(9)	.1649(1)	-.2341(3)	0.8(1)
O(21-1)	-.1130(20)	.1991(11)	-.3463(26)	4.6(4)
O(21-1m)	.1249(11)	.1985(6)	-.3393(11)	0.3(1)
O(21-2)	-.0042(17)	.0796(4)	-.2794(9)	2.1(1)
O(21-3)	.0057(23)	.1912(4)	-.0110(10)	2.2(1)
Si(22)	.0043(8)	.3364(1)	.2831(3)	0.8(1)
O(22-1)	-.1219(11)	.2900(6)	.2500(11)	0.6(1)
O(22-1m)	.1198(14)	.2850(7)	.2699(15)	2.0(2)
O(22-2)	.0127(14)	.3969(3)	.1015(8)	1.3(1)
O(22-3)	-.0006(17)	.3760(3)	.4934(8)	1.2(1)

* Estimated standard errors refer to the last digit.

The refined site occupancies are X(11) = 0.707(6)Ca + 0.293(6)Ba; M(11) = 0.64(1)Mg + 0.36(1)Mn; M(12) = 0.93(1)Mg + 0.07(1)Mn; and Y(11) = 0.88(3)Ca + 0.12(3)Mg.

[1] For a copy of the structure factor data, Table 5, order Document AM-75-010-A from the Business Office, Mineralogical Society of America, 1909 K Street, N. W. 20006. Please remit in advance $1.00 for the microfiche.

TABLE 3. Bredigite. Anisotropic Thermal Vibration Parameters for the Alkaline Earth Cations *X*, *Y*, and *M**

Atom	β_{11}	β_{22}	β_{33}	β_{12}	β_{13}	β_{23}
X(11)	48.8(1.9)	12.3(0.6)	50.2(2.6)	0.0	0.0	6.8(0.9)
X(12)	53.7(2.9)	6.4(0.7)	51.8(3.6)	0.0	0.0	-3.1(1.5)
X(21)	14.7(2.7)	4.9(0.8)	41.2(4.4)	4.0(1.4)	-3.0(2.6)	-2.7(1.4)
X(22)	18.1(3.0)	10.0(1.0)	52.7(4.7)	1.0(1.5)	-8.5(2.9)	0.0(1.6)
M(11)	12.4(3.0)	5.9(0.9)	45.6(4.8)	0.0	0.0	3.0(1.7)
M(12)	7.5(3.6)	3.6(1.1)	22.8(5.9)	0.0	0.0	-0.7(2.0)
Y(11)	27.2(3.1)	10.7(1.1)	65.0(5.9)	-4.1(1.7)	-2.1(4.2)	9.3(1.7)
Y(12)	29.8(2.6)	6.7(0.9)	33.4(4.3)	-7.3(1.4)	-13.8(3.5)	-7.4(1.4)
Y(21)	30.8(1.8)	9.2(0.6)	58.4(2.9)	-5.2(1.9)	2.0(5.0)	-0.4(1.0)
Y(22)	21.3(1.7)	16.2(0.6)	55.3(2.8)	-6.9(2.1)	9.0(5.0)	3.9(1.1)

*Coefficients in $\exp-\left[\beta_{11}h^2 + \beta_{22}k^2 + \beta_{33}\ell^2 + 2\beta_{12}hk + 2\beta_{13}h\ell + 2\beta_{23}k\ell\right]$.

sis, since the distributions of the alkaline earths between the two phases is unknown. We shall discuss this point further on. We shall also show that the correlation between site distributions and average polyhedral Me–O distances is good and that the refined site distributions are probably fairly sensible.

One cosmetically unappealing aspect of the refined thermal vibration parameters are the differences between oxygen pairs of the kind O(*pq-r*) and O(*pq-rm*). This symbolism is explained further on—suffice it to state here that these pairs are atoms which would be equivalent if the mirror planes were in fact present. Since the average *B* values between these pairs are similar to the averages for the individual tetrahedra, we feel that the sufficiently high correlations in atomic coordinate parameters are the cause for differences in the vibration parameters between atom pairs related by pseudosymmetry. Their individual bond distances indicate that their actual atomic coordinates are probably close to the true values and we are not too upset about the differences in *B* values expressed in Table 2.

Discussion on the bredigite structure

Topology of the structure: combinatorial crystal structures

The general outline of the bredigite problem proceeds directly from Moore's (1973) study, which organized the structural relationships among calcium orthosilicate and alkali sulfate structures on combinatorial mathematical grounds. Four types of polyhedra were discerned: $X^{[12]}$, a truncated rhombohedron; $Y^{[10]}$, a polar polyhedron whose upper hemisphere is related to the cuboctahedron, $F^{[12]}$; and the tetrahedron, $T^{[4]}$. The $X^{[12]}$ polyhedron can be conceived as a trigonal antiprism with six additional meridional vertices approximately coplanar with the central cation. The maximum coordination number which obtains, $X^{[12-p]}$ where $0 \leq p \leq 6$, is defined by the orientations of the circumjacent tetrahedra.

For $p = 6$, all tetrahedral apices point away from the central cation and the coordination polyhedron reduces to the central trigonal antiprism, which is identified as the octahedron, $M^{[6]}$. Intermediate values of p are determined by the "bracelet" type, as defined by Moore (1973). There are sixteen discrete bracelets but three include chiral pairs, so there exist thirteen topological types (see Appendix I for the enumeration of these arrangements by a counting theorem). Depending on the topological type, a value can be assigned to p, and this value determines the meridional vertices of $X^{[12]}$ which are occupied by coordinating oxygens.

The bracelet types are the heart of the problem. They can be joined to generate an infinite number of possible periodic arrangements, and each arrangement thus obtained can be transformed into the *ideal* structure by associating the corresponding structural unit, or "pinwheel," with each bracelet. Actually, the use of the bracelets and pinwheels is a very powerful tool since all discrete arrangements or structure types can be retrieved for any cell shape or symmetry class and the cumbersome construction of the *ideal* structure can be circumvented, at least before the final comparison between the ideal structure and the real one is desired. The patterns of linked bracelets are in effect directly related to the

TABLE 4. Bredigite. Parameters for the Ellipsoids of Vibration for the Alkaline Earth Cations *X*, *Y*, and M*

	i	μ_i (x10^2)	θ_{ia}	θ_{ib}	θ_{ic}
X(11)	1	17.2	0	90	90
	2	9.9	90	111	21
	3	15.0	90	159	111
X(12)	1	18.0	0	90	90
	2	9.7	90	38	52
	3	11.6	90	52	142
X(21)	1	11.7	130	129	65
	2	6.7	132	42	84
	3	9.3	113	103	154
X(22)	1	13.2	102	167	83
	2	9.1	39	95	51
	3	12.1	53	102	140
M(11)	1	11.0	90	48	42
	2	8.7	0	90	90
	3	9.2	90	42	132
M(12)	1	7.9	90	158	68
	2	6.7	0	90	90
	3	7.1	90	112	158
Y(11)	1	15.7	116	41	60
	2	9.9	109	130	46
	3	12.3	147	98	122
Y(12)	1	15.2	149	60	82
	2	1.9	64	54	47
	3	11.7	75	50	136
Y(21)	1	15.0	37	127	85
	2	10.8	127	141	82
	3	11.6	91	99	171
Y(22)	1	17.5	111	21	86
	2	8.4	138	109	54
	3	12.5	124	99	144

* μ_i = r.m.s. amplitude of the i-th principal axis. The θ values are the angles between the i-th axis and the crystal axes a, b and c.

combinatorial problem of enumerating discrete populations on the hexagonal net, {6, 3}.

Another advantage gained from the condensation of bracelets to form a periodic array is that the ideal space group of the bracelet configurations corresponds exactly to the space group of the ideal structure. Transformation of any array of linked bracelets into some nonisomorphic bracelet array will be defined as a *topological distortion.* A topological distortion creates a new ideal structure. Distortion of any ideal structure into the real structure will be called a *geometrical distortion.* These terms appear natural since a topological change implies change in the ideal coordination number for the $X^{[12-p]}$ polyhedra whereas a geometrical distortion implies some continuous movement away from the ideal coordination. The latter necessarily leads to lower coordination numbers whereas the former may result in either higher or lower coordination numbers.

Moore and Araki (1972) and Moore (1973) have emphasized that merwinite, $Ca_3Mg[SiO_4]_2$, is a geometrical distortion of the glaserite ($P\bar{3}m1$) structure type and that larnite, β-$Ca_2[SiO_4]$, is a geometrical distortion of room temperature β-$K_2[SO_4]$. The ideals of these two structures are topologically distinct. The ideal structure type for bredigite appears to be an arrangement new to scientific intelligence; its bracelet condensation is shown in Figure 1, and the ideal structure in Figure 2. Its cell parameters relative to bredigite (Fig. 3) are $a' = a/2$; $b' = b$; $c' = c$, and the space group is $P2/m2_1/c\ 2_1/b$. Its ideal formula can be written $X^{[12]}X_2^{[9]}Y_4^{[10]}M^{[6]}[TO_4]_4$. This immediately suggests that the ideal upper limit in Mg content for bredigite is $Ca_7Mg[SiO_4]_4$. Analogous to merwinite, which is $X^{[12]}Y_2^{[10]}M^{[6]}[TO_4]_2 (= Ca_3Mg[SiO_4]_2)$, ideal bredigite probably has a fixed Ca:Mg ratio which is dictated by the presence of the $M^{[6]}$ octahedra. In merwinite, the MgO_6 octahedra are linked at corners by the tetrahedra to form sheets (Moore and Araki, 1972); in bredigite, they link by the tetrahedra to form chains which run parallel to the *a* axis. We conclude that bredigite is in fact a novel structure type and not a geometrical distortion of either the glaserite or the β-$K_2[SO_4]$ structure types. The β-$K_2[SO_4]$ ideal is $X^{[9]}Y^{[10]}[TO_4]$ and its larnite distortion evidently does not admit Mg^{2+} into its structure owing to the absence of a true octahedral coordination but instead having maximal coordinations higher than 6.

Then what is the relationship between α'-$Ca_2[SiO_4]$ and bredigite? Douglas, in a detailed and very careful study on bredigite, stated "This observation, however, does *not* establish the identity of bredigite and α'-$Ca_2[SiO_4]$, since visual comparison of the two powder photographs shows some marked differences in the two patterns." Despite this caution, most authors accept an identity between the two (see Biggar, 1971, who presents a good historical outline on the problem). On the basis of phase equilibrium studies, Biggar (1971) states "Bredigite is used for a phase of unknown composition range, probably between $(Ca_{1.80}Mg_{0.20})SiO_4$ and $(Ca_{1.70}Mg_{0.30})SiO_4$ . . .". In other words, the formula unit is bracketed between $Ca_{7.2}Mg_{0.8}[SiO_4]_4$ and $Ca_{6.8}Mg_{1.2}[SiO_4]_4$. We feel com-

TABLE 6. Bredigite. Polyhedral Interatomic Distances*

X(11)			
Antiprism			
2 X(11)	-	O(21-2)	2.38
2	-	O(12-1)	2.86
2	-	O(11-1m)	2.88
average			2.71
Meridion			
2 X(11)	-	O(11-3)	2.82
2	-	O(12-3)	3.01
2	-	*O(21-3)*	*3.51*
average			2.91
$X(11)^{[10]}$	grand average		2.79
$X(11)^{[12]}$	grand average		(2.91)

X(12)			
Antiprism			
2 X(12)	-	O(11-1)	2.40
2	-	O(12-1m)	2.51
2	-	$O(22\text{-}2)^{ii}$	*3.29*
average			2.45
Meridion			
2 X(12)	-	$O(22\text{-}3)^{ii}$	2.28
2	-	*O(12-3)*	*3.41*
2	-	*O(11-3)*	*3.52*
average			2.28
$X(12)^{[6]}$	grand average		2.40
$X(12)^{[12]}$	grand average		(2.90)

M(11)			
Antiprism			
2 M(11)	-	O(22-2)	2.02
2	-	$O(12\text{-}1m)^{ii}$	2.11
2	-	$O(11\text{-}1)^{ii}$	2.22
average			2.12
Meridion			
none			

M(12)			
Antiprism			
2 M(12)	-	$O(11\text{-}1m)^{ii}$	2.00
2	-	$O(21\text{-}2)^{ii}$	2.08
2	-	$O(12\text{-}1)^{ii}$	2.12
average			2.07
Meridion			
none			

X(21)			
Antiprism			
X(21)	-	$O(22\text{-}1)^{ii}$	2.31
	-	$O(21\text{-}1)^{ii}$	2.36
	-	$O(11\text{-}2)^{ii}$	2.43
	-	O(22-1m)	2.45
	-	O(12-2)	2.59
	-	O(21-1m)	2.65
average			2.46
Meridion			
X(21)	-	O(12-3)	2.52
	-	O(21-3)	2.61
	-	*$O(22\text{-}3)^{ii}$*	*3.45*
average			2.56
$X(21)^{[8]}$	grand average		2.49
$X(21)^{[9]}$	grand average		(2.60)

X(22)			
Antiprism			
X(22)	-	$O(22\text{-}1m)^{ii}$	2.32
	-	O(22-1)	2.32
	-	$O(21\text{-}1m)^{ii}$	2.36
	-	O(11-2)	2.43
	-	$O(12\text{-}2)^{ii}$	2.43
	-	O(21-1)	2.73
average			2.43
Meridion			
X(22)	-	O(11-3)	2.56
	-	O(21-3)	2.63
	-	*$O(22\text{-}3)^{ii}$*	*3.48*
average			2.59
$X(22)^{[8]}$	grand average		2.47
$X(22)^{[9]}$	grand average		(2.58)

Si(11)		
Si(11)	-O(11-3)	1.58
	-O(11-2)	1.61
	-O(11-1m)	1.61
	-O(11-1)	1.65
average		1.61
O(11-1)-O(11-1m)		2.59
O(11-2)-O(11-3)		2.60
O(11-2)-O(11-1m)		2.61
O(11-2)-O(11-1)		2.63
O(11-3)-O(11-1m)		2.63
O(11-3)-O(11-1)		2.73
average		2.63

Si(12)		
Si(12)	-O(12-1m)	1.59
	-O(12-3)	1.60
	-O(12-1)	1.65
	-O(12-2)	1.65
average		1.62
O(12-2)-O(12-1)		2.54
O(12-2)-O(12-1m)		2.60
O(12-3)-O(12-1)		2.61
O(12-2)-O(12-3)		2.66
O(12-1)-O(12-1m)		2.66
O(12-3)-O(12-1m)		2.78
average		2.64

Y(11)			
Apex			
Y(11)	-	$O(11\text{-}3)^{ii}$	2.30
Base			
Y(11)	-	$O(11\text{-}1m)^{ii}$	2.53
	-	$O(11\text{-}2)^{ii}$	2.71
	-	*$O(11\text{-}1)^{ii}$*	*3.12*
average			2.62
Meridion			
Y(11)	-	$O(21\text{-}1)^{ii}$	2.46
	-	$O(11\text{-}1)^{iii}$	2.53
	-	$O(21\text{-}2)^{ii}$	2.66
	-	O(22-2)	2.69
	-	$O(11\text{-}1m)^{iii}$	2.83
	-	O(22-1m)	2.85
average			2.67
$Y(11)^{[9]}$	grand average		2.62
$Y(11)^{[10]}$	grand average		(2.67)

Y(12)			
Apex			
Y(12)	-	$O(12\text{-}3)^{ii}$	2.23
Base			
Y(12)	-	$O(12\text{-}2)^{ii}$	2.66
	-	$O(12\text{-}1)^{ii}$	2.67
	-	*$O(12\text{-}1m)^{ii}$*	*3.00*
average			2.66
Meridion			
Y(12)	-	$O(12\text{-}1m)^{iii}$	2.39
	-	$O(21\text{-}1m)^{ii}$	2.48
	-	O(22-1)	2.67
	-	O(22-2)	2.85
	-	$O(21\text{-}2)^{ii}$	2.87
	-	*$O(12\text{-}1)^{iii}$*	*3.06*
average			2.65
$Y(12)^{[8]}$	grand average		2.60
$Y(12)^{[10]}$	grand average		(2.69)

Y(21)			
Apex			
Y(21)	-	O(21-3)	2.33
Base			
Y(21)	-	O(21-1)	2.59
	-	O(21-1m)	2.61
	-	*O(21-2)*	*3.13*
average			2.60
Meridion			
Y(21)	-	O(11-2)	2.43
	-	O(22-1m)	2.44
	-	O(22-1)	2.64
	-	O(11-1m)	2.72
	-	*O(12-2)*	*3.11*
	-	*O(12-1)*	*3.16*
average			2.56
$Y(21)^{[7]}$	grand average		2.54
$Y(21)^{[10]}$	grand average		(2.72)

Y(22)			
Apex			
Y(22)	-	$O(21\text{-}3)^{ii}$	2.21
Base			
Y(22)	-	$O(22\text{-}2)^{ii}$	2.33
	-	*$O(22\text{-}1)^{ii}$*	*3.44*
	-	*$O(22\text{-}1m)^{ii}$*	*3.52*
average			2.33
Meridion			
Y(22)	-	O(11-2)	2.33
	-	O(12-2)	2.34
	-	O(11-1)	2.95
	-	$O(21\text{-}1)^{ii}$	2.97
	-	$O(21\text{-}1m)^{ii}$	2.97
	-	O(12-1m)	3.03
average			2.77
$Y(22)^{[8]}$	grand average		2.64
$Y(22)^{[10]}$	grand average		(2.81)

Si(21)		
Si(21)	-O(21-3)	1.58
	-O(21-2)	1.60
	-O(21-1)	1.61
	-O(21-1m)	1.62
average		1.60
O(21-1) -O(21-2)		2.53
O(21-1m)-O(21-3)		2.57
O(21-1) -O(21-1m)		2.59
O(21-1) -O(21-3)		2.61
O(21-1m)-O(21-2)		2.63
O(21-2) -O(21-3)		2.73
average		2.61

Si(22)		
Si(22)	-O(22-1m)	1.58
	-O(22-3)	1.59
	-O(22-1)	1.63
	-O(22-2)	1.65
average		1.61
O(22-1m)-O(22-3)		2.60
O(22-1m)-O(22-2)		2.62
O(22-1) -O(22-3)		2.63
O(22-1m)-O(22-1)		2.64
O(22-1) -O(22-2)		2.65
O(22-2) -O(22-3)		2.67
average		2.63

*Distances beyond those accepted for real coordination number are italicized. They are parenthetically included in the interatomic polyhedral average. The upper limit to estimated standard deviations in distances is Me–O ±0.02Å and O–O′ ±0.03Å.

i = +, -, -; ii = 1/2+, 1/2-, 1/2+; iii = 1/2+, 1/2+, 1/2- applied to atomic coordinates in Table 2.

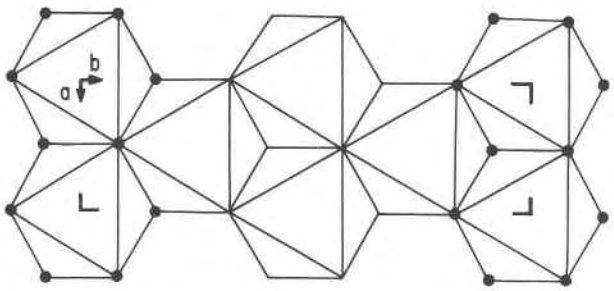

FIG. 1. Condensed bracelets within the unit cell of the *Pmcb* ideal structure about the $z = 0$ level. Solid circles are the p extra coordinations for $X^{[6+p]}$.

pelled to propose that bredigite is in fact a stoichiometric compound with composition $CaMg[SiO_4]_4$ just as merwinite is a stoichiometric compound with composition $Ca_3Mg[SiO_4]_2$. Since there is no evidence which suggests significant deviations in merwinite stoichiometry, we believe that bredigite, too, is a well-ordered compound which requires a smaller octahedral cation to stabilize its structure. The α'-$Ca_2[SiO_4]$, therefore, is most likely yet another structure type or a distinctly different geometrical distortion of the presently established ones; a single crystal study on α'-$Ca_2[SiO_4]$ toward elucidation of its structure is a task which should be accepted with utmost urgency[2]. Further on, we shall show that powder photographs alone afford insufficient information for correctly establishing the structure type of any of these phases and that patterns with significant differences must be treated with great caution before mutual identity is proposed.

The key feature which appears to define ordered compounds involving Mg^{2+} or other divalent cations of similar radius is a structure ideal which involves the $M^{[6]}$ polyhedron, that is, $X^{[12]-p]}$ stripped of its p-equatorial vertices. This is achieved through only one kind of pinwheel, that of Figure 5b in Moore (1973). In this pinwheel, the tetrahedral apical oxygens point as far away as possible from the central cation.

We shall discuss the group-subgroup relations among topologically and geometrically transformed bracelet condensations in relation to the actual bredigite structure. There exists only one ideal arrangement in which the bredigite cell shape and the space group *Pmnn* obtains; it is featured as Figures 10 and 11 in Moore (1973). Its ideal composition is $X^{[12]}X^{[10]}X_4^{[9]}X^{[8]}Y_8^{[10]}M^{[6]}[TO_4]_8$ or $Ca_{15}Mg[SiO_4]_8$. It, too, is a distinct structure type. By selecting larger and larger cells in the plane, an infinite number of possible arrangements can be conceived (the easiest demonstration of this is to take the hexagonal net and stepwise add solid disks to form discrete bracelet arrangements). Thus, the discrete bracelet condensations imply that these structures are "infinitely adaptive" in the sense used by Anderson (1973). To emphasize this point we inquired how many arrangements can be found which belong to either space group *Pmcb* or $Pm2_1b$ and which fulfill a bredigite-shaped cell or a subcell ($a' = a/2$). Enumeration and discussion of these arrangements appears in Appendix II. Three of these belong to space group *Pmcb* and the remaining nine belong to $Pm2_1b$. It is evident that even the criteria of cell contents and space group are insufficient to distinguish structure types and that detailed study of some unknown phase requires the careful examination of the individual single crystal X-ray intensities. Geometrical distortion of the structure ideal, of course, adds a further complication to the problem.

The parent space group to which the calcium orthosilicate structures can be pulled out as subgroups is $P6_3/m\ 2/m\ 2/c$ (see Eysel, 1973, for an excellent discussion on the system Na_2SO_4–K_2So_4–K_2CrO_4–Na_2CrO_4). The immediate orthorhombic maximal symmetry subgroup is $C2/m\ 2/c\ 2_1/m$. By doubling b and selecting the appropriate equivalent point set, $P2/m\ 2_1/c\ 2_1/b$ results. In effect, the hexagonal parent group contains all tetrahedra in a disordered configuration (simultaneous up (u) and down (d)). This primitive orthorhombic group is obtained by ordering the (u, d) arrays in the condensed bracelet, and it obtains from a *topological distortion*. Doubling a and inducing a *geometrical distortion* leads to $P2/m\ 2_1/n\ 2_1/n$. Finally, the mirror plane is destroyed by another geometrical distortion leading to *P2nn*.

The space group genealogy is offered in Table 7. Thus, bredigite obtains from one topological distortion followed by two kinds of geometrical distortion of the parent space group $C2/m\ 2/c\ 2_1/m$. It involves two "klassengeich" subgroup relations and one "zellengleich" subgroup (see Neubüser and Wondratschek, 1966, for a discussion on the genealogy of space groups).

Bredigite from the Middlesbrough slags is a highly ordered compound. From Tilley and Vincent (1948) its cell contents can be rewritten $Ca_{24.6}Ba_{1.2}Mg_{4.8}Mn_{1.4}[SiO_4]_{16}$, assuming a 2:1 ratio between the larger cations and the tetrahedral cat-

[2] During construction of this manuscript, a preprint by H. Saalfeld (1975) was brought to our attention. In that study, Saalfeld studied α'-$Ca_2[SiO_4]$ single crystals at high temperature. His results indicate structures derived from the *Pnma* parent space group of β-$Ca_2[SiO_4]$ and not the *Pmcb* parent group of bredigite.

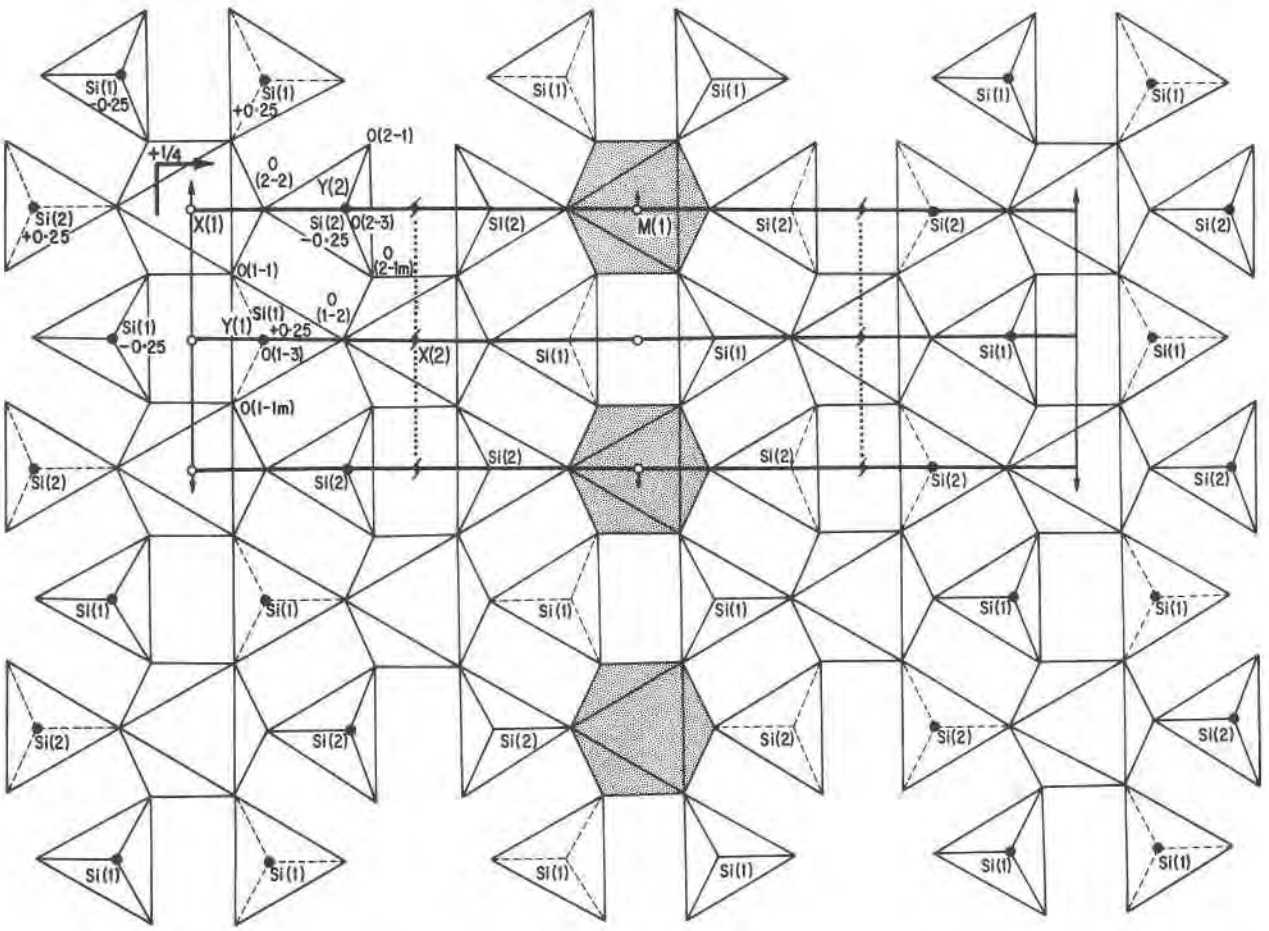

FIG. 2. Structure ideal for the *Pmcb* arrangement to which bredigite is related. The symmetry elements and the unit cell are outlined. This obtains from the condensed bracelets in Figure 1. The nonequivalent atom positions are labelled, and the octahedral sites are stippled.

ions. These authors express some uncertainty about bredigite's composition owing to the presence of impurities in the slag. Accepting our site population refinement (Table 2), the cell contents in the bredigite crystal would be $Ca_{26.9}Ba_{0.6}Mg_{3.6}Mn_{0.9}[SiO_4]_{16}$; it is not known, however, what the partitioning of cations is between bredigite and the trigonal phase. Despite these uncertainties, our structure analysis has already shown that Ba is preferentially ordered over the $X(11)$ sites at 000, *etc*; and Mn over the $M(11)$ site at 0, 1/2, 0, *etc*. Such an ordering scheme doubles the *a'* axis of the $P2/m\ 2_1/c\ 2_1/b$ group and leads to $P2/m\ 2_1/n\ 2_1/n$. Destruction of the mirror plane is achieved by twisting or tilting of the tetrahedra away from special positions along $(0\ y\ z)$ and $(1/2\ y\ z)$. These ordering schemes, based on substituent cations of different ionic radii, were postulated by Moore (1973) although in that paper it was argued that a large Ba^{2+} cation would prefer a *Y* site. Evidently, with the large $X^{[12]}$ site available, the Ba^{2+} cation can achieve even higher coordination. As a consequence of this ordering, the $X(11)$ site in the real structure is approximately 10-coordinated and $X(12)$ is reduced to approximate 6-coordination although the latter is not an octahedron. In the ideal structure both sites are $X^{[12]}$. As for the geometrical distortion leading to lower average coordination than the ideal model, the twisting or tilting of the tetrahedra away from the mirror planes follows from Moore (1973): "The explanation appears to be a matter of compromise between *ideal* geometry and *actual* coordination number." Bond distances and their distortions are pursued in greater detail in the next section.

This detailed analysis suggests that the crystal chemistry of bredigites may in fact be more complicated than expected. For example, in the pure

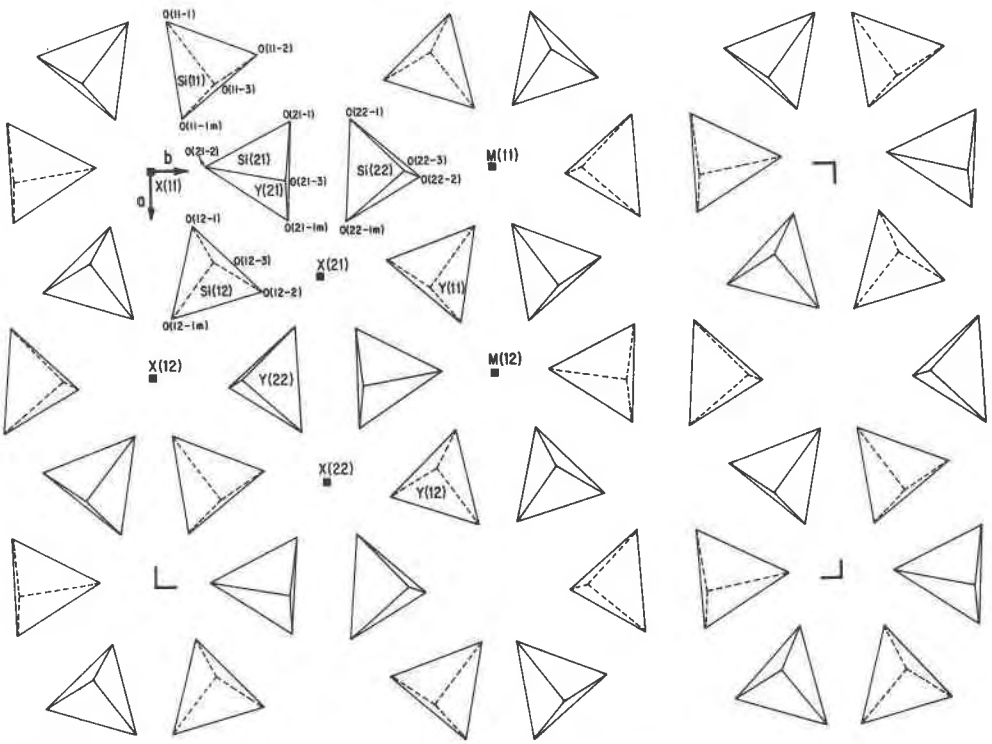

FIG. 3. Dispositions of the tetrahedra in the real bredigite structure. Non-equivalent atoms are labelled in accordance with Figure 2 and Table 2.

$Ca_7Mg[SiO_4]_4$ compound, it is conceivable that the space group remains $P2/m\ 2_1/c\ 2_1/b$ with a halving of the bredigite *a* axis. It is also possible, however, that distortion leading to lower symmetry may occur just as pure larnite is a distorted β-$K_2[SO_4]$ structure (in the larnite structure, the mirror plane is destroyed). It is conceivable that the composition $BaCa_6Mg[SiO_4]_4$ may be stable in the $P2/m\ 2_1/c\ 2_1/b$ group: here, $X(11) = X(12) =$ Ba; $M(11) = M(12) =$ Mg, with no distinction between distortions in $X(11)$ and $X(12)$, or $M(11)$ and $M(12)$. Attempts at growth of single crystals at these compositions and their detailed crystallographic study should prove a further fruitful investigation. On this note, it is conceivable that the hypothetical ideal *Pmnn* structure (earlier written as $Ca_{15}Mg[SiO_4]_8$) may in fact be stabilized by exploiting the $X^{[12]}$–$X^{[10]}$ · · · chain along the *a* direction, *i.e.*, with a composition $BaCa_{14}Mg[SiO_4]_8$.

From these conjectures, studies of bredigite over a temperature range must be approached with great caution since it is possible that continuous changes in the distortions will drive the space group toward the parent supergroups. In addition, the $X^{[12]}$ polyhedron itself is highly adaptive and allows a range of coordination numbers through continuous geometrical distortion.

Detailed analysis of bond distances

A tabulation of bond distances for bredigite will not suffice without a nomenclature that links the *X*, *Y*, *M*, and *T* polyhedra to the ideal $P2/m\ 2_1/c\ 2_1/b$ group. This can be easily achieved if the reader is willing to accept a slightly cumbersome labelling scheme. The ideal structure (Fig. 3) has the following cationic sites in the asymmetric unit: *X*(1), *M*(1), *Y*(1), *Y*(2), Si(1) and Si(2). The anions are labelled according to their coordinated cations: thus, Si(1) has O(1–1), O(1–1m), O(1–2), and O(1–3) (it is convenient to write O(1–1) and O(1–1*m*) in such a way to show their equivalence by reflection in the ideal structure). In general, anions in the actual bredigite structure will be written O(*pq–r*) and O(*pq–rm*), where *p* refers to the parent ideal structure, *q* the nonequivalence created in the actual bredigite structure, and *r* and *m* adopt the same relation as expressed above. Locations of the non-equivalences in the ideal and real structures are provided in Figures 2 and 3.

Next, it is necessary to compute all the Me–O distances for the maximum coordination permitted by the ideal structure. Thus, in Table 6 the discrete cations and their maximum permitted coordinations

are $X(11)^{[12]}$, $X(12)^{[12]}$, $M(11)^{[6]}$, $M(12)^{[6]}$, $X(21)^{[9]}$, $X(22)^{[9]}$, $Y(11)^{[10]}$, $Y(12)^{[10]}$, $Y(21)^{[10]}$, $Y(22)^{[10]}$, $Si(11)^{[4]}$, $Si(12)^{[4]}$, $Si(21)^{[4]}$, and $Si(22)^{[4]}$. The X-polyhedral distances include six trigonal anti-prismatic distances and the $(6-p)$ meridional distances; the Y polyhedral distances include four to the tetrahedra above and below (vertex + base) and the remaining six meridional distances. Inspection of these distances reveals the actual distortions away from ideality for the bredigite crystal.

The problem then reduces to assigning the *real* coordination number to a cation. Since the distances in Table 6 are arranged in ascending values, a cutoff value must be selected. The longest values (those which are excluded from the real coordination) tend to be separated by a definite break at around 3.0 Å. For all the Y polyhedra, the bonds to the tetrahedral apex are the shortest. The basal bonds and the meridional bonds, however, do not contrast in any obvious manner. For the X polyhedra, the antiprismatic bonds tend to be shorter on the average than the meridional bonds but even here no hard and fast rule is observed (see $X(12)$ where distortions are particularly severe). One of the interesting aspects of this kind of analysis is that some consistency in average polyhedral bond distances appears. The proposed *real* coordination numbers are: $X(11) = 10$; $X(12) = 6$; $X(21) = X(22) = 8$; $M(11) = M(12) = 6$; $Y(11) = 9$; $Y(12) = Y(22) = 8$, and $Y(21) = 7$. Based on these, the average distances are: $X(11)$–O 2.79 Å; $X(12)$ 2.40 Å; $X(21)$ 2.49 Å; $X(22)$ 2.47 Å; $M(11)$ 2.12 Å; $M(12)$ 2.07 Å; $Y(11)$ 2.62 Å; $Y(12)$ 2.60 Å; $Y(21)$ 2.54 Å; $Y(22)$ 2.64 Å.

The $X(11)$–O = (0.71 Ca+ 0.29 Ba)–O calculated average, from the tables of Shannon and Prewitt (1969) is 2.75 Å and clearly confirms the preferential occupancy of Ba^{2+} cations over the $X(11)$ site in the structure. The $M(11)$–O = (0.64 Mg + 0.36 Mn)–O is significantly longer than the $M(12)$–O = Mg–O average and supports the preferential site occupancy of Mn^{2+} in the former position. Average distances for Ca–O are $Ca^{[6]}$–O 2.40 Å, $Ca^{[7]}$–O 2.47 Å, $Ca^{[8]}$–O 2.52 Å, $Ca^{[9]}$–O 2.58 Å, and $Ca^{[10]}$–O 2.68 Å according to Shannon and Prewitt. These values do not depart seriously from those found in bredigite. In merwinite, the averages are $Ca(1)^{[8]}$–O 2.56 Å, $Ca(2)^{[9]}$–O 2.59 Å, and $Ca(3)^{[8]}$–O 2.58 Å, values which are practically the same as those found for bredigite. The refined structure of bredigite also suggests that minor Mg^{2+} (12%) substitutes for Ca^{2+} in the $Y(11)$ site. If this substitution is indeed real, then the bredigite composition may depart somewhat from ideal $Ca_7Mg[SiO_4]_4$ in real crystals. The preferential and complete occupancy of Mg^{2+} and similar smaller cations over the $M(11)$ and $M(12)$ positions has been clearly established, however.

TABLE 7. Genealogy of the Pinwheel Structures

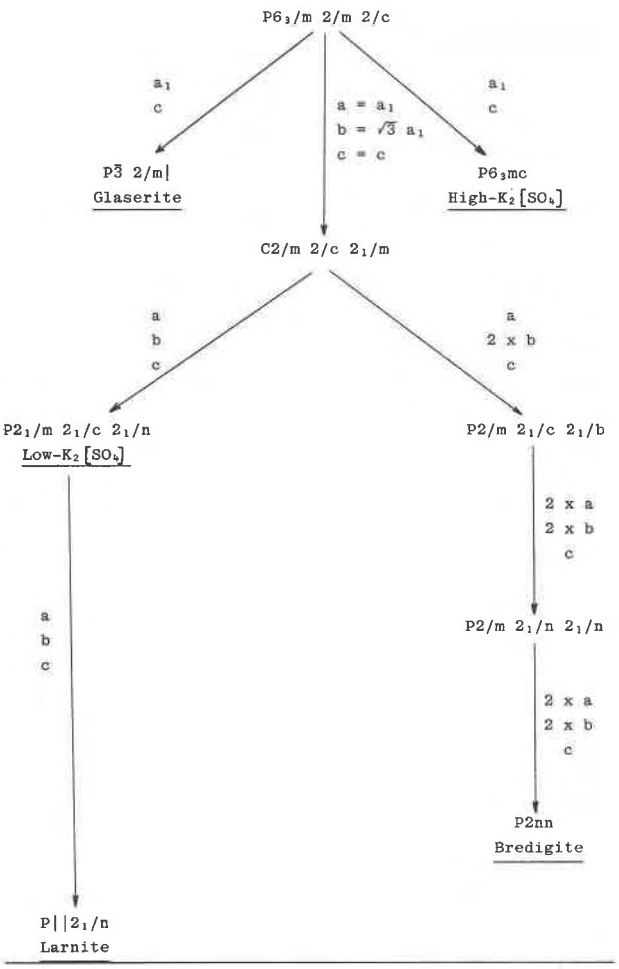

The preferential occupancy of Ba^{2+} in the $X(11)$ position must be accepted as an essential aspect of bredigite chemistry and may in fact be required for stability of its structure. This implies that the ideal limits in bredigite compositions for crystals in *P2nn* space group are between $Ca_{14}Mg_2[SiO_4]_8$ and $BaCa_{13}Mg_2[SiO_4]_8$, the latter where $X(11)$ is completely occupied by Ba^{2+}.

More problems: Bredigite-like powder patterns

Since the true structure of bredigite has been shown to be derived by geometrical distortion of the *Pmcb* ($a' = a/2$, $b' = b$, $c' = c$) ideal structure, it

should be possible to directly obtain the ideal coordinates of the atoms which correspond to those in bredigite. These ideal coordinates are presented in Table 8; when compared with those of the refined bredigite structure a striking similarity is seen, the deviations being at most not over 1 Å. This suggests that powder and even single crystal intensity data may be very similar even though the structures are different. The *Pmnn* ideal structure (Fig. 11 of Moore, 1973) is topologically distinct from that of the ideal *Pmcb*. How do these structures affect the intensity data? Is there even a likelihood that topologically distinct structures may in fact afford similar powder patterns? If so, the problems in distinguishing discrete phases are amplified since it has been shown that the ideal structures are the basis for the determination of coordination numbers, hence the kinds of ionic species which may or may not substitute over non-equivalent alkaline earth sites.

In Figure 4, calculated powder intensities for Fe$K\alpha_1$ radiation are plotted versus 2θ for merwinite (A), the refined bredigite structure (B), the *Pmcb* ideal (C) and the *Pmnn* ideal (D). For these calculations, the scattering curves assigned to the alkaline earth sites were Mg^{2+} for $M^{[6]}$ and Ca^{2+} for the $X^{[12-p]}$, with Si^{4+} and O^{2-} assigned to the remainder. All four reveal remarkable similarities in their intensity distributions, merwinite showing the most pronounced difference from the rest. For the patterns B, C, and D, the most pronounced similarities are found between 2θ = 40-45° and in many of the higher angle clusters, such as between 2θ = 75-80°. The most conspicuous differences appear in the low angle regions, especially below 2θ = 20°. Since the structures involve a sizable number of non-equivalent positions, distortions are averaged out at high angles while the low-angle reflections are sensitive to cation ordering and short range distortions. In many respects, these calculated power patterns *more resemble each other* than do the diagrammatic X-ray diffraction patterns for bredigite, *T*-type silicate, α'-$Ca_2[SiO_4]$, and β-$Ca_2[SiO_4]$ featured in Biggar (1971). The recent work of Saalfeld (1975) leads us to conclude that α'-$Ca_2[SiO_4]$ and bredigite are distinct phases; and larnite (β-$Ca_2[SiO_4]$) is a derivative of room temperature $K_2[SO_4]$ according to Midgley (1952) and Moore (1973). The status of the "*T*-type silicate" remains uncertain: this may be yet another structure type or a pure version of bredigite. A recent paper by Saalfeld (1974) reports a = 10.945 Å, b = 18.393 Å, c = 6.747 Å, space group *Pmnn* for the "*T* phase" grown by the Verneuil method. This suggests a close relationship between the "*T* phase" and bredigite, but it will be necessary to compare single crystal intensities of the two before a definite conclusion can be advanced.

TABLE 8. Bredigite. Atomic Coordinate Parameters from Ideal Model*

	x	y	z		x	y	z
X(11)	.00	.00	.00	Si(12)	.25	.08	.25
X(12)	.50	.00	.00	O(12-1)	.13	.04	.32
				O(12-1m)	.37	.04	.32
X(21)	.25	.25	.00	O(12-2)	.25	.17	.32
X(22)	.75	.25	.00	O(12-3)	.25	.08	.00
M(11)	.00	.50	.00				
M(12)	.50	.50	.00				
				Si(21)	.00	.17	-.25
Y(11)	.25	.42	.17	O(21-1)	-.12	.20	-.32
Y(12)	.75	.42	.17	O(21-1m)	.12	.20	-.32
				O(21-2)	.00	.08	-.32
Y(21)	.00	.17	.33	O(21-3)	.00	.17	.00
Y(22)	.50	.17	.33				
Si(11)	.75	.08	.25	Si(22)	.00	.33	.25
O(11-1)	.62	.04	.32	O(22-1)	-.12	.30	.18
O(11-1m)	.87	.04	.32	O(22-1m)	.12	.30	.18
O(11-2)	.75	.17	.32	O(22-2)	.00	.32	.18
O(11-3)	.75	.08	.00	O(22-3)	.00	.33	.50

* *Refer to Figure 2. The coordinates are based on the bredigite cell and can be compared with Table 2.*

Recommendations for further research

The detailed crystal chemistry in the system $CaO–MgO–SiO_2$ is clearly a very complex problem, yet it is merely one aspect of the general problem of the "bracelet and pinwheel structures." Even the apatite structure type can be conceived as a pinwheel-type structure (Moore, unpublished manuscript). These structures can be found among phases in the system $Na_2O–BaO–P_2O_5$, $Na_2O–CaO–P_2O_5$, $CaO–SiO_2–P_2O_5$, $K_2O–Na_2O–SO_3$ as well. With broad-range goals in mind, the following suggestions are made, any one of which will lead to fruitful research.

1. Stabilized high temperature structure types

The crystal chemical study on merwinite (Moore and Araki, 1972) and the present study on bredigite indicate that high-temperature structure types are probably stabilized through the *ordering* of large (such as Ba^{2+}) and small (such as Mg^{2+}) cations over select non-equivalent positions which inhibit inversion to low temperature structures upon quenching. The evidence is also strong that the addition of alkaline earth cations other than Ca^{2+} leads to fairly stoichiometric compounds despite the relatively high Ca:Mg ratio. Bredigite is one such example. The bond strengths for Mg–O are sufficiently strong to afford a kinetic barrier, assuring the preservation of the high temperature structure type.

Studies should be made toward the delineation of

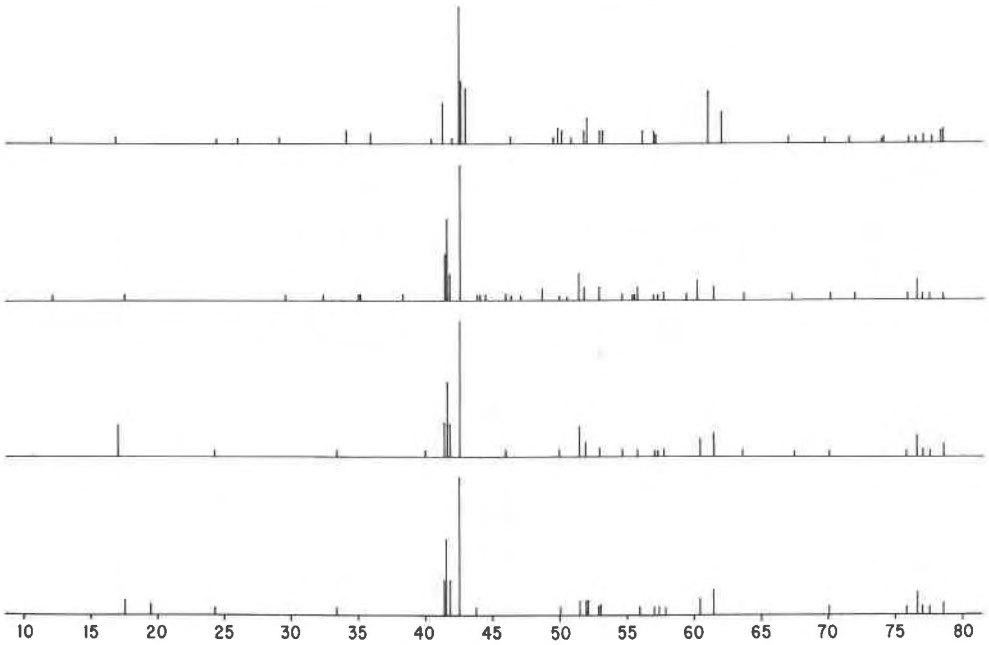

FIG. 4. Calculated power patterns from top to bottom: merwinite (A), refined bredigite (B), the *Pmcb* ideal (C), and the unique *Pmnn* ideal (D). 2θ for Fe$K\alpha$ radiation is along the abscissa.

stoichiometric compounds in the system K_2O–Na_2O–BaO–CaO–MgO–Al_2O_3–SiO_2–P_2O_5–SO_3–H_2O and its subsystems. At present, many investigators are concentrating on two- and three-component subsystems but few are integrating these seemingly separate systems into a unified whole.

2. *Detailed crystal chemistry of the structure types*

Despite the enormous literature on phase-equilibria and on determinative tools, especially powder diffraction, our knowledge of the structure types is at best meager. Few structures have been solved in detail and even fewer well-refined. But little is known about site occupancies for "stabilized" phases. Although some of this stems from the inherent difficulty of the problem and the necessity for *in situ* high temperature diffraction studies, much of the problem rests on the reluctance on the part of many investigators to attempt growth of suitable single crystals for detailed structure analysis. A powerful and fruitful technique appears in the link between the detailed structure analysis results with those of powder diffraction, both experimental and calculated. Here, a well-refined structure is crucial.

Owing to the similarities among the discrete pinwheel structures, even the single crystal results have to be approached with much care and caution. Since several topologically distinct structure types could conceivably provide the same cell criteria (including space groups), careful attention to the intensity distributions is required.

3. *Continuous structural distortions: displacive versus reconstructive phase transitions*

It appears that distortions of the structure of the geometrical type correspond to displacive phase changes, whereas topological distortions (*i.e.*, discrete bracelet ideals) are reconstructive. For the latter, however, continuous geometrical deformation can lead to a "hybrid" polyhedron, that is, one in which the topological ideal is not clearly recognized. For example, the $X^{[12]}$ and $F^{[12]}$ polyhedra can be related to each other by $\pi/6$ radian rotations about an axis normal to opposing pairs of triangular faces. The $X^{[12]}$ polyhedron is a 3-connected system whereas $F^{[12]}$ is 4-connected. A rotation by $\pi/12$ radians leads to a polyhedron which shares properties of both. It is clear that rotations of the $X^{[12]}$ and $F^{[12]}$ polyhedra define rotations of the tetrahedra in the real structure so that the distinction between geometrical and topological distortions is admittedly not sharp, at least within a certain range of distortion.

Although there does not appear be any ambiguity in relating larnite to the room temperature $K_2[SO_4]$

structure, bredigite to the *Pmcb* ideal, and merwinite to glaserite, a displacive-type phase-change is less clear. Does this proceed continuously or does it proceed in discrete steps? In other words, are the $X^{[12-p]}$ polyhedra deformed by continuous rotations (which presumably can be related to temperature) or are there "jumps" in the *real* coordinations of these polyhedra with respect to their ideals?

Acknowledgments

Professor S. O. Agrell provided the valuable Middlesbrough type specimen of Tilley and Vincent and on numerous occasions ferreted out other specimens peripheral to this study. The importance of having type material for the basis of extended study cannot be underestimated. On several occasions, Professor P. J. Wyllie and Dr. Wuu-Liang Huang synthesized crystals of related compounds, materially adding to some of the conclusions in this paper. Dr. H. Saalfeld submitted a preprint of his study on α'-$Ca_2[SiO_4]$, thus circumventing any gross speculations about the relationship between bredigite and this phase.

It is a pleasure to acknowledge financial support from the N.S.F. GA-40543 grant, and the N.S.F. Materials Research Laboratory grant awarded to The University of Chicago.

Appendix I

Enumeration of the thirteen discrete bracelets for the trigonal antiprism

Let the domain $D(d_1, \cdots d_6)$ correspond to the six vertices of the trigonal antiprism and the range $R(b,p)$ corresponds to the two possible entries on those vertices, either a solid disk (b) or an empty slot (p) (see Moore, 1973, p. 36). The permutation group, $G(\pi_1, \cdots \pi_6)$, corresponds to the enantiomorphic crystal class {32}.

The cycle index is $P\{32\} = \frac{1}{6}(X_1^6 + 2X_3^2 + 3X_2^3)$ and the pattern inventory is $F\{32{:}b,p\} = b^6 + b^5p + 4b^4p^2 + 4b^3p^3 + 4b^2p^4 + bp^5 + p^6$. Thus, there are sixteen discrete arrangements.

Consider now the permutation group $G(\pi_1, \cdots \pi_{12})$ corresponding to the holosymmetric crystal class $\{\bar{3}\ 2/m\}$. The cycle index is $P\{\bar{3}\ 2/m\} = \frac{1}{12}(X_1^6 + 4X_2^3 + 3X_1^2X_2^2 + 2X_3^2 + 2X_6^1)$ and the pattern inventory is $F\{\bar{3}\ 2/m{:}b,p\} = b^6 + b^5p + 3b^4p^2 + 3b^3p^3 + 3b^2p^4 + bp^5 + p^6$. Thus, there are thirteen discrete arrangements.

Now $F\{32{:}b,p\} \supset F\{\bar{3}\ 2/m{:}b,p\}$. This is seen in the pattern inventories since b^4p^2, b^3p^3 and b^2p^4 each contains a chiral mate. Thus, three of the thirteen discrete arrangements must include three objects belonging to enantiomorphic crystal classes.

The arrangements are summarized in Table 9. The analysis of pattern inventories adopts the convention of Liu (1968) the origins of which can be found in Pólya (1937).

It is noted that the bracelets are related in complementary way with the complements of b^rp^s found in b^sp^r. For b^rp^r, the bracelets are self-complements.

TABLE 9. Pattern Inventory for the Bracelets*

	b^6	b^5p	b^4p^2		
New symbol	b^6	b^5p	b^4p^2 (1)	b^4p^2 (2)	b^4p^2 (3)
Old symbol	(3+3)c	(4+2)c	(3+3)a´	(5+1)a	(3+3)b´
Point group	$\bar{3}$ 2/m	m	2/m	m	2
	p^6	bp^5	b^2p^4		
New symbol	p^6	bp^5	b^2p^4 (1)	b^2p^4 (2)	b^2p^4 (3)
Old symbol	(3+3)c´	(4+2)c´	(3+3)a	(5+1)a´	(3+3)b
Point group	$\bar{3}$ 2/m	m	2/m	m	2
		b^3p^3			
New symbol		b^3p^3 (1)	b^3p^3 (2)	b^3p^3 (3)	
Old symbol		(6+0)a	(4+2)a	(4+2)b	
Point group		3m	m	1	

*The new symbol shall be the bracelet symbol adopted in this study. It is based on the number of coordinating meridional vertices (b) and the number of empty vertices (p), where p is used in the same sense as $X^{[12-p]}$. The old symbol appears in Moore (1973) and is based on tetrahedra pointing either up (u) or down (d). The advantages of the new symbolism are (1) it follows directly from a counting theorem and, (2) the cumbersome use of u's and d's can be avoided.

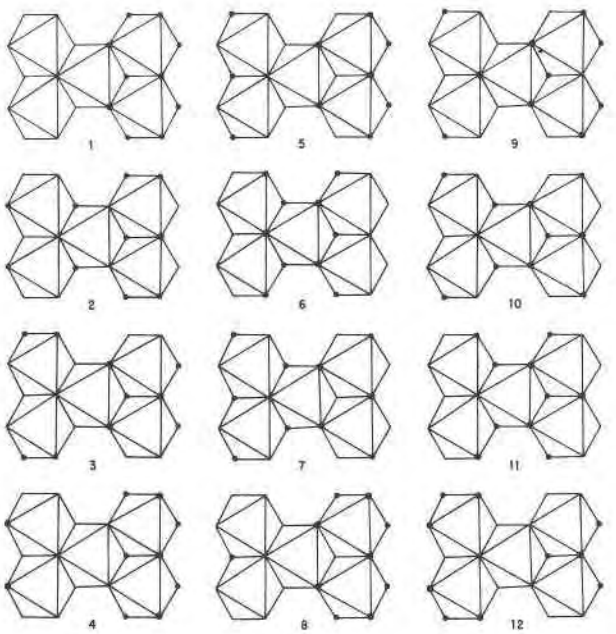

FIG. 5. The half- or quarter-cell units for the twelve condensed bracelets which conform to bredigite-like cells and subcells in space groups *Pmcb* and $Pm2_1b$.

Appendix II

Retrieval of structures containing bredigite-like cells and subcells in space groups Pmcb and $Pm2_1b$

The following cell shapes are admissible with respect to the bredigite a, b, and c dimensions: $a' = a$ or $a/2$; $b' = b$; $c' = c$. Both space groups require a mirror plane normal to the a direction and a $b/2$-glide normal to the c' direction. Thus, complements of the bracelets at $(x\ y\ z)$ appear at $(x, 1/2+y, z)$. The space group *Pmcb* requires, in addition, a two-fold rotation axis parallel to the a' direction. The twelve arrangements are shown as half- or quarter-cell $(a'/2, b'/2)$ units in Figure 5.

(a) *The condition $a' = a/2$, Pmcb.* Two arrangements obtain. They

must be based on bracelets containing point symmetry $2/m$. Arrangement 1 (Fig. 5) is the ideal of bredigite; arrangement 2 is a discrete structure type.

(b) *The condition $a' = a$, Pmcb.* One arrangement (3) obtains. It must be based on the bracelets with point symmetry 2. Note that arrangements (1) and (2) through a "klassengleich"-type distortion can also fulfill condition (b).

(c) *The condition $a' = a/2$, $Pm2_1b$.* Four arrangements (4, 5, 6, 7) obtain and these are based on bracelets with point symmetry m. Note that (4) and (5) are novel arrangements and that (6) and (7) are in fact "zellengleich" distortions of (1) and (2).

(d) *The condition $a' = a$, $Pm2_1b$.* Five arrangements (8, 9, 10, 11, 12) can be found which possess lower symmetry and which have not been previously retrieved.

It is informative to inquire of the ideal coordinations for the X polyhedra in these structures. They are: $X^{[12]}X_2^{[9]}M^{[6]} = 1, 6$; $X_2^{[11]}X_2^{[7]} = 4$; $X^{[11]}X^{[10]}X^{[8]}X^{[7]} = 8, 10, 11$; $X^{[11]}X_2^{[9]}X^{[7]} = 12$; $X^{[10]}X_2^{[9]}X^{[8]} = 2, 3, 7$; and $X_2^{[10]}X_2^{[8]} = 5, 9$.

References

ANDERSON, J. S. (1973) On infinitely adaptive structures. *J. Chem. Soc.* (Dalton Trans.) **1973,** 1107–1115.

BIGGAR, G. M. (1971) Phase relationships of bredigite $Ca_5MgSi_3O_{12}$ and of the quaternary compound ($Ca_6MgAl_8SiO_{21}$) in the system CaO–MgO–Al_2O_3–SiO_2. *Cement and Concrete Res.* **1,** 493–513.

BUSING, W. R., K. O. MARTIN, AND H. A. LEVY (1962) ORFLS, a Fortran crystallographic least-squares program. *U.S. Natl. Tech. Inform. Serv.* **ORNL-TM-305.**

CROMER, D. T., AND D. LIBERMAN (1970) *Los Alamos Scientific Laboratory, Univ. Calif. Rep.* **LA-4403, UC-34.**

———, AND J. B. MANN (1968) X-ray scattering factors computed from numerical Hartree-Fock wave-functions. *Acta Crystallogr.* **A24,** 321–324.

DOUGLAS, A. M. B. (1952) X-ray investigation of bredigite. *Mineral. Mag.* **29,** 875–884.

EYSEL, W. (1973) Crystal chemistry of the system Na_2SO_4–K_2SO_4–K_2CrO_4–Na_2CrO_4 and of the glaserite phase. *Am. Mineral.* **58,** 736–747.

FINGER, L. W. (1969) Determination of cation distribution by least-squares refinement of single crystal X-ray data. *Carnegie Inst. Wash. Year Book,* **67,** 216–217.

LIU, C. L. (1968) *Introduction to Combinatorial Mathematics.* McGraw-Hill, Inc., New York, p. 147–161.

MIDGLEY, C. M. (1952) The crystal structure of β-dicalcium silicate. *Acta Crystallogr.* **5,** 307–312.

MOORE, P. B. (1973) Bracelets and pinwheels: a topological-geometrical approach to the calcium orthosilicate and alkali sulfate structures. *Am. Mineral.* **58,** 32–42.

———, AND T. ARAKI (1972) Atomic arrangement of merwinite, $Ca_3Mg[SiO_4]_2$, an unusual dense-packed structure of geophysical interest. *Am. Mineral.* **57,** 1355–1374.

NEUBÜSER, J., AND H. WONDRATSCHEK (1966) Untergruppen der Raumgruppen. *Kristall. u. Technik.* **1,** 530–543.

PÓLYA, G. (1937) Kombinatorische Anzalbestimmungen für Gruppen, Graphen, und chemische Verbindungen. *Acta Math.* **68,** 146–254.

RAMACHANDRAN, G. N., AND R. SRINIVASAN (1970) *Fourier Methods in Crystallography.* Wiley-Interscience, New York, p. 96–119.

SAALFELD, H. (1974) Kristallographische Untersuchungen über die Verbindung $Ca_7MgSi_4O_{16}$ (phase T) im System Ca_2SiO_4–$Ca_3Mg(SiO_4)_2$. *Ber. Deutsch. Keram. Gesell.* **51,** 295–298.

——— (1975) X-ray investigation of single crystal β-Ca_2SiO_4 (larnite) at high temperature. *Am. Mineral.* **60,** 824–827.

SHANNON, R. D., AND C. T. PREWITT (1969) Effective ionic radii in oxides and fluorides. *Acta Crystallogr.* **B25,** 925–946.

TILLEY, C. E., AND H. C. G. VINCENT (1948) The occurrence of an orthorhombic high temperature form of Ca_2SiO_4 (bredigite) in the Scawt Hill contact-zone and as a constituent of slags. *Mineral. Mag.* **28,** 255–271.

ZACHARIASEN, W. H. (1968) Experimental tests of the general formula for the integrated intensity of a real crystal. *Acta Crystallogr.* **A24,** 212–214.

Manuscript received, April 3, 1975; accepted for publication, June 27, 1975.